Hindawi
Shock and Vibration
Volume 2022, Article ID 7412777, 11 pages
https://doi.org/10.1155/2022/7412777

Research Article

Blasting Vibration Law and Prediction in the Near-Field of Tunnel

Meng Wang,[1] **Weijie Ding**,[1] **Dakai Zhao**,[1] **Dianshu Liu**,[1] **Lukai Wang**,[1] **Tao Zhang**,[1] **and Tianlong Ling**[2]

[1]*School of Mechanics and Civil Engineering, China University of Mining & Technology (Beijing), Beijing 100083, China*
[2]*College of Mechanical and Architecture Engineering, Taishan University, Tai'an 271000, China*

Correspondence should be addressed to Meng Wang; wangmeng12316@163.com

Received 10 December 2021; Accepted 1 March 2022; Published 20 March 2022

Academic Editor: Xiao Wang

The stability of surrounding rock near the tunnel face is very important to the safety of constructors and the tunnel itself. The vibration law of surrounding rock obtained from the vibration data in the far-field of tunnel blasting is not suitable for the near-field. Therefore, in order to guarantee the safety of tunnel drilling and blasting, it is important to study the vibration law of surrounding rock near the tunnel face. Taking Zhaitang Tunnel, the New Line Expressway of China National Highway 109, as the engineering background, acceleration sensors were installed in the surrounding rock near the tunnel face to test the blasting vibration acceleration of the surrounding rock at the arch waist of the tunnel, to study the blasting vibration attenuation law near the large section tunnel, to modify traditional blasting vibration formula, and to improve the vibration prediction accuracy. The research will bring some guidance for the construction of similar projects.

1. Introduction

Too much attention has been paid to the influence of blasting seismic waves on distant buildings. However, the safety of blasting near the blasting source is also very important in blasting construction. For example, in the process of tunnel blasting construction, the blasting source is close to the tunnel support structure or the protected target, sometimes only a few meters away, which will cause more serious blasting vibration problems. At present, there has been relatively mature research on the dynamic response in far-field. However, based on the effective information obtained far from the blasting source, it is impossible to correctly describe the impact of explosion load on buildings (structures) and materials in the near-field of blasting source only with the experience obtained by analysis and prediction of the action in the near-field of tunnel, and it can even produce large errors [1]. Therefore, figuring out the attenuation law and vibration characteristics of explosion waves near the blasting source is of great significance to further reveal the blasting failure mechanism and ensure the safety construction of tunnel blasting [2–4].

Yang et al. monitored the vibration attenuation in the rock mass 2–15 m near the blasting holes and concluded that the vibration amplitude predicted by the traditional prediction formula was significantly lower than the measured value [1]. Holmberg and Persson put forward an improved integral formula of particle vibration velocity in the near-field of open-pit blasting [5]. Fleetwood studied the vibration attenuation law of single-hole waveform of open-pit and established a bivariate polynomial vibration prediction model based on a large number of test data [6]. Zhang et al. also found that the particle vibration velocity in the near-field of blasting does not conform to the law obtained from the vibration data in the far-field of blasting [7]. Zhang took the bedrock excavation blasting of the Three Gorges Dam as the background and obtained the blasting vibration law in the near-field of blasting. He also used the neural network theory to establish the blasting vibration prediction model and determine the boundary of the rock blasting loose crack area and the critical particle vibration velocity range of the bedrock [8, 9]. Based on the concrete model test, Ye et al. took a preliminary study of the energy distribution and attenuation characteristics of the near-field and far-field of

the concrete under blasting [10]. Fu et al. used customized large-scale velocity sensors in the surrounding rock of the arch crown installed during the excavation of the pilot tunnel to monitor the vibration and studied the vibration law in the near-field [11–13]. Zhang proposed applying proportional distance to tunnel zoning and using BP wavelet neural network to predict near-field vibration blasting [14]. Xie et al. used Anderson linear superposition model to simulate vibration in the process of cut blasting according to single-hole waveform in the near-field of a tunnel, established a prediction model of near-field vibration velocity, and also verified its feasibility through engineering practice [15, 16]. Han studied the vibration characteristics near the blasting area of an open-pit mine and made a prediction of it with Anderson linear superposition model [17, 18]. In recent years, due to the excessive damage of surrounding rock near the working face, the falling of arch crown rock blocks or the collapse of primary lining concrete blocks occur from time to time, damaging the on-site equipment and seriously threatening the life safety of constructors [19–22].

In view of this, Zhaitang Tunnel, the New Line Expressway of China National Highway 109, is selected for blasting vibration monitoring to study the characteristics and laws of near-field vibration of tunnel. In addition, in order to solve the safety problem of tunnel near-field vibration, the vibration prediction formula suitable for tunnel blasting near-field is revised and verified.

2. Experimental Details

2.1. Site Background. National Highway 109 is located in Mentougou District, Beijing, with a length of 65.455 km and a designed speed limit of 80 km/h. The entire expressway is divided into 11 work areas; among them, the 9th work area is located in Zhaitang Town and Qingshui Town (both in Mentougou District, Beijing). The main construction projects of the 9th work area are two tunnels of Zhaitang 1# and Zhaitang 2#. The construction layout of the 9th work area is presented in Figure 1.

The mileage of the left line of Zhaitang 1# tunnel ranges from AK51 + 750 to AK 54 + 381, with a length of 2631 m. The tunnel is a separate double-track four-lane tunnel, and one lane is reserved for the two lanes of the main tunnel (the pavement width is 12.75 m). At the small mileage ends of the left and right lines of Zhaitang 1# tunnel, the longitudinal gradient of 700 m is 1.28%; the remaining of 1925 m is 2.00% and the transverse gradient is 3%.

2.2. Geological Conditions. The surrounding rocks of Zhaitang 1# tunnel are mainly andesite and andesitic breccia lava. In which sandstone, silty sand, and shale are distributed, and coal seams are exposed. The surrounding rock is mainly graded V and IV and locally grade III. The state of surrounding rock is relatively broken to broken, and the stability of it is poor.

2.3. Blasting Patterns. AK52~AK53 section of Zhaitang 1# tunnel is selected for the test in this paper. The test section is grade III surrounding rock with good rock conditions. The cutting hole adopts compound-wedge cutting mode, the hole bottom is ultradeep by 0.2 m; 8 pairs of cutting holes are arranged, and advance per round of 3.5–4.0 m was set up. The electronic detonator is used for sectional initiation, and the interval time is set as 50 ms or 70 ms. The blasting sequence is as follows: the cutting hole is detonated first; and then the caving hole is detonated from the inner ring hole to the outer ring hole, followed by the peripheral hole; and the bottom plate hole is detonated finally. The blast hole layout is illustrated in Figure 2.

In order to ensure the construction progress, the two-step method was adopted for the excavation. Because the working faces' spacing of the upper and lower steps is about 60 m; the upper step has the characteristics of full-face blasting. According to the actual blasting effect on-site, the blasting scheme was timely and flexibly adjusted (Table 1).

The cutting hole, caving hole, and bottom hole shall be charged with explosive continuously and detonated sectionally, while interval charging was adopted for peripheral holes. The diameter of all the holes is φ42 mm. The selected cartridge is 2# rock emulsion explosive with diameter of φ32 mm and density of 1.0 g/cm3. All holes were detonated at the bottom of the hole.

2.4. Vibration Monitoring. Blasting vibration near-field monitoring brings great challenges due to the limited construction space and complex near-field environment in the tunnel. Flying rocks and smoke from blasting may damage monitoring instruments and affect subsequent work. In view of the problems existing in the test process, a new monitoring method is adopted in this field test: the sensor is embedded in the surrounding rock and installed in the boreholes 0.5 m and 1.0 m deep at the arch waist. Furthermore, to avoid the interference of construction of vibration test and establish the tunnel excavation face near-field blasting vibration monitoring system for tunnel stability and real-time monitoring of blasting vibration signals, the wiring, inspection, recycling, and a lot of work have been to reduce a lot, and lots of protection measures are adopted such as vibration isolation vibration; wire PVC pipe is used to protect the transmission lines; special protection box is used to protect the acquisition instrument, and so on. The instrument installation scheme and details are shown in Figures 3 to 5.

According to Wang et al.'s research, the properties of epoxy resin mortar as filling material are close to natural rock, which can reduce the error caused by dynamic matching [23]. When arranging the measuring points, the X-axis of the sensor points to the tunnel face (horizontal tangential), the Y-axis points to the tunnel radial (horizontal radial), and the Z-axis points to the tunnel tangential (vertical) (Figures 6 and 7).

Compared with the speed sensor, the acceleration sensor has the advantages of small volume, light weight, convenient installation, and high sensitivity. Especially when monitoring large-scale blasting activities, the acceleration sensor is more suitable for selection because of its large range and wide-frequency response range. The ULT2010-500 IEPE

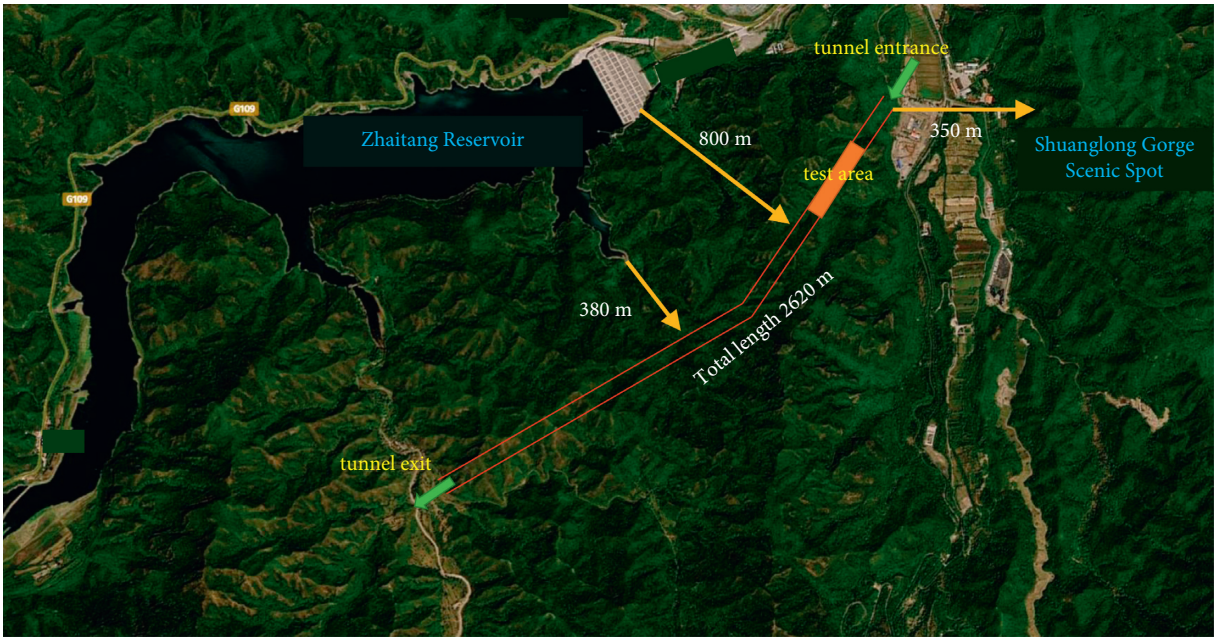

Figure 1: Schematic diagram of Zhaitang 1# tunnel.

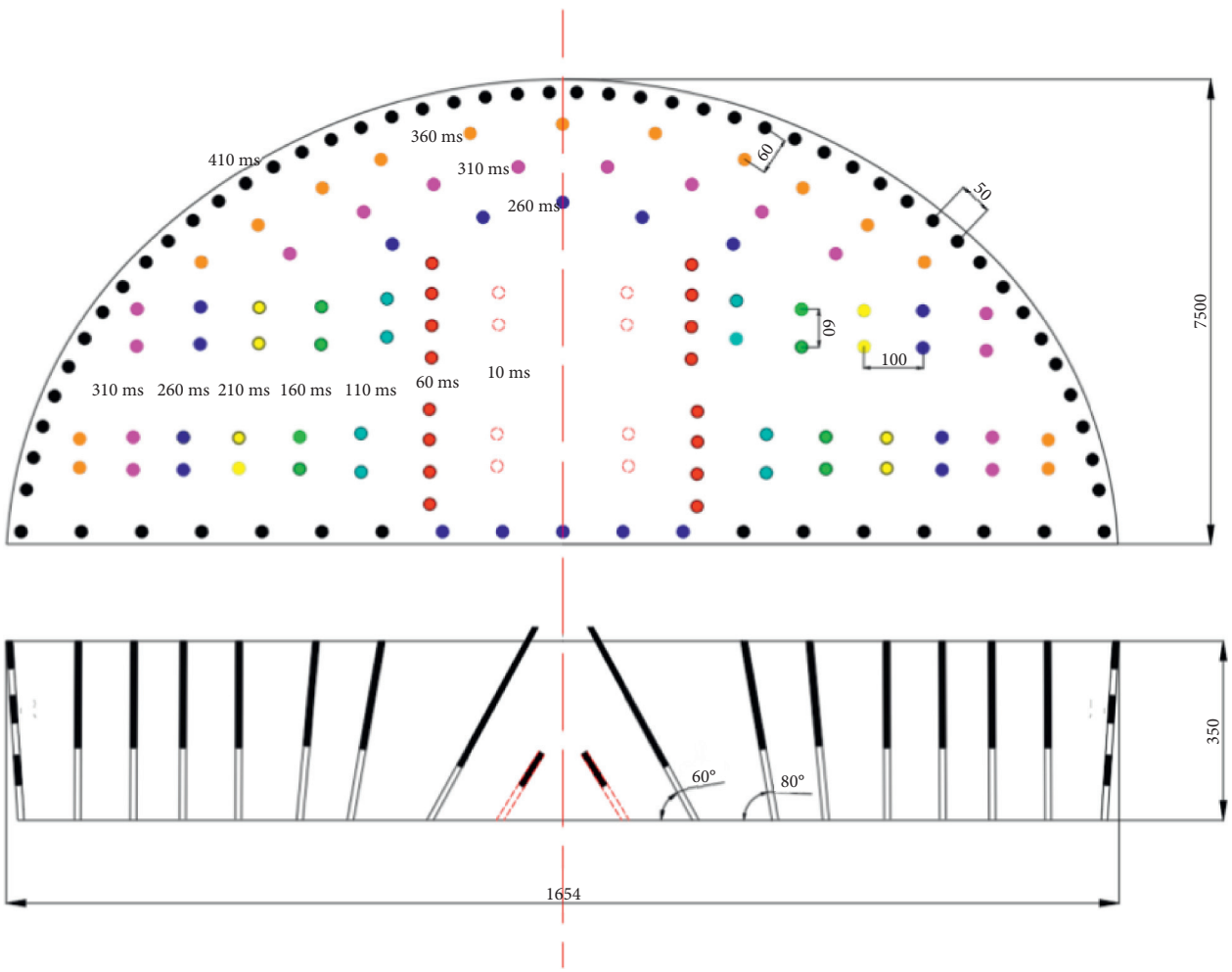

Figure 2: Layout of blast holes on the upper steps of the right line tunnel (unit: mm).

Table 1: Blasting parameters of upper bench of tunnel.

Type of blasting hole	Delay time (ms)	Numbers	Depth (m)	Charge per hole (kg)	Charge (kg)
Cut hole	10	6	3	1	6
	60	16	4.7	3.3	52.8
Caving hole	110	8	4.5	3	24
	160	8	4.3	2.4	19.2
	210	8	4	2.4	19.2
	260	13	4	2.4	52
	310	16	4	2.4	38.4
	360	8	4	2.4	19.2
		13	4	1.8	23.4
Peripheral hole	410	25	1	0.4	10
		50	4	1	50
Bottom hole	260	5	4	3.6	18
	410	12	4	3.6	43.2
Total		188			375.4

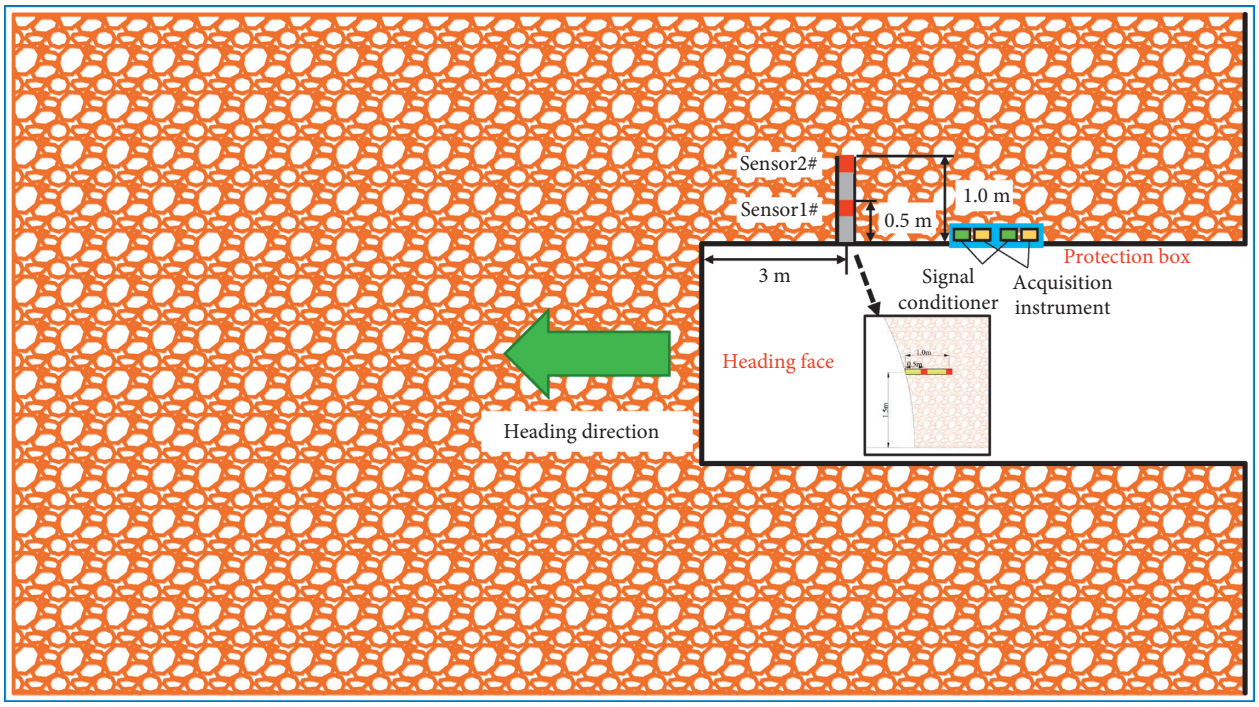

Figure 3: Blasting vibration monitoring scheme.

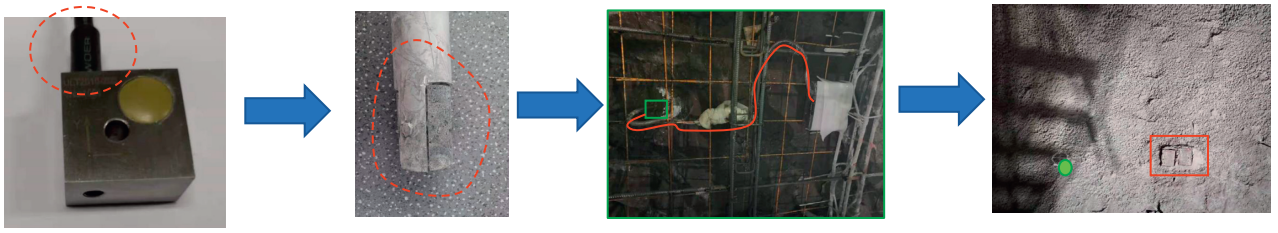

(1) Waterproof treatment (2) Pouring and cutting (3) Field installation (4) Shotcreting

Figure 4: Sensor installation process.

piezoelectric acceleration sensor of LANCETEC company is selected for this test, with a range of 0–500 g, a frequency response range of 0.5–5000 Hz, and a sensitivity of 10 mV/g. IEPE acceleration sensor needs to be used together with the signal conditioner to provide constant current supply. The output signal of the sensor is directly isolated and transformed into a standard voltage signal for signal acquisition and analysis by the later-stage data collector. CM3503™

Figure 5: Site layout scheme of vibration measuring instrument.

Figure 6: ULT2010-500 triaxial acceleration sensor.

Figure 7: TC-4850 vibration acquisition instrument.

three-channel conditioner is selected, which can output ±10 V voltage, provides 4 mA constant current source to supply the sensor, and has 1 or 10 times gain amplification instrumentation. TC-4850 blasting vibration instrument developed by Chengdu Zhongke Measuring and Controlling Co., Ltd., is used in the test. The A/D resolution of the equipment is 16 bits, the maximum analog input is 10 V, and Figure 8 the sampling frequency is 1–50 kHz.

3. Blasting Vibration Characteristics

3.1. Typical Waveform Analysis. For the test data of section AK52 + 257, two representative typical waveforms are selected for analysis. The near-field waveform is 3 m away from the tunnel face, with a total charge of 367 kg. The far-field waveform is 132.5 m away from the tunnel face, and the total charge is 370 kg.

It can be seen from Figures 9 and 10 that the near-field waveform has the characteristics of obvious segmentation, short duration, high frequency, and large peak value, while the far-field vibration has the characteristics of waveform superposition, long duration, low frequency, and small peak value. When the blast holes at different positions are detonated successively, multiple vibration signals with certain time difference are generated in the near blasting area, showing obvious waveform separation. With the increase of the propagation distance, the vibration duration becomes longer, and the waveforms of different segments, amplitudes, frequencies, and phases are superimposed to form a composite wave.

The tunnel excavation adopts multisegments and millisecond-level blasting. In this project, the delay time is divided into eight segments: the cutting holes are the first segment, the caving holes are the second to seventh segments, and the peripheral holes and some bottom holes are the eighth segments. However, during the actual construction, the blasting scheme will need to be properly adjusted according to the specific situation, such as adding small cutting holes (primary cutting) or caving holes.

During tunnel blasting excavation, in order to obtain the blasting vibration waveform of each section as independently as possible, the initial interval of 50 ms is adjusted to 70 ms. There is basically no superposition of blasting vibration waveforms in the near and middle field. But with the increase of distance, when it reaches about 100 m, the blasting waveform begins to be partially superimposed. Therefore, in blasting vibration tests,

Figure 8: CM3503™ three-channel signal conditioner.

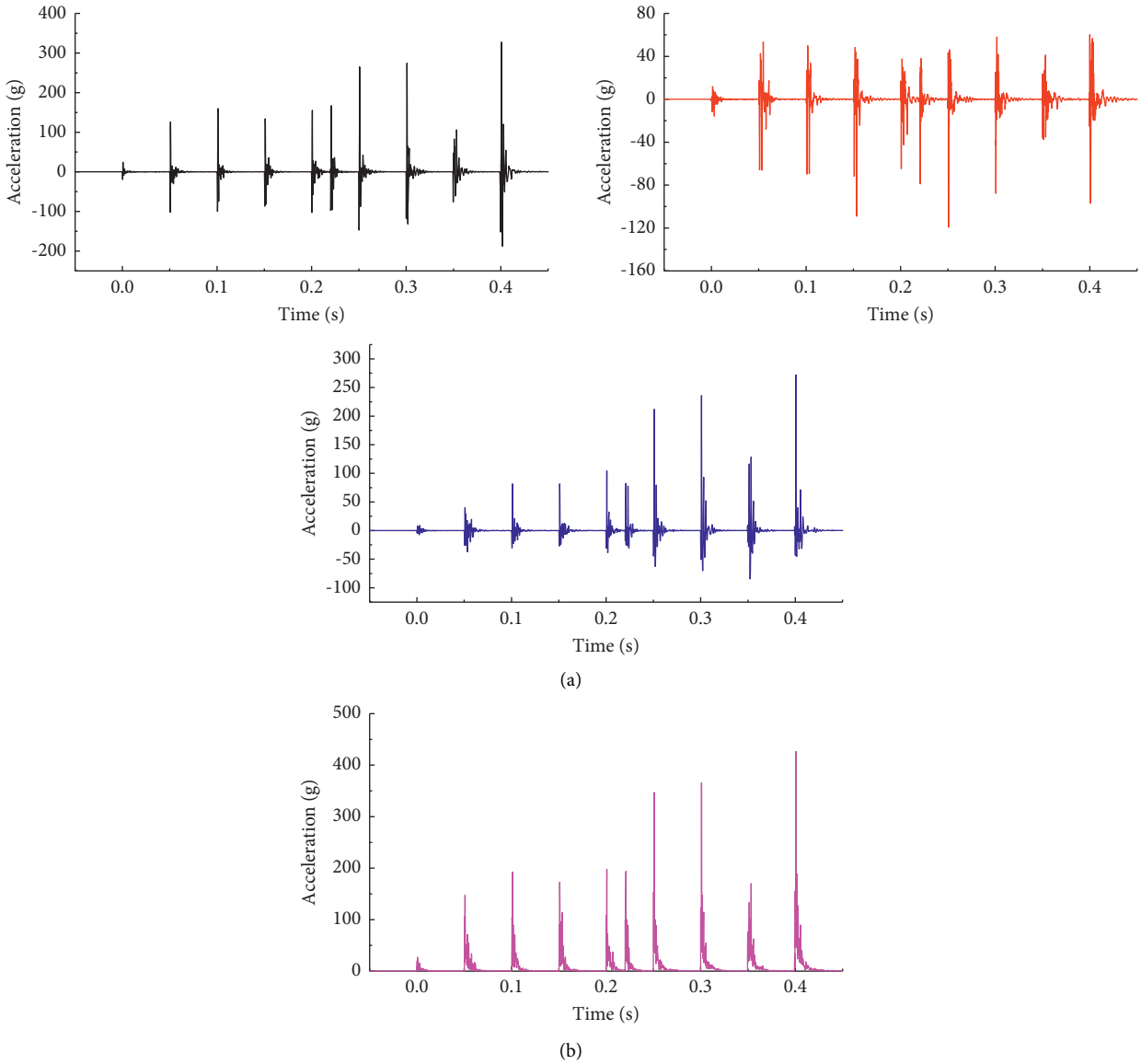

Figure 9: Acceleration waveform at 3m near tunnel face. (a) Three-direction waveform of blasting vibration acceleration. (b) Total acceleration waveform.

appropriate monitoring distance shall be selected according to the blasting scheme so as to obtain the separated waveform for analysis.

3.2. Division of Tunnel Blasting Area. Before selecting the components of the blasting vibration monitoring system, it is necessary to define the distance range of blasting

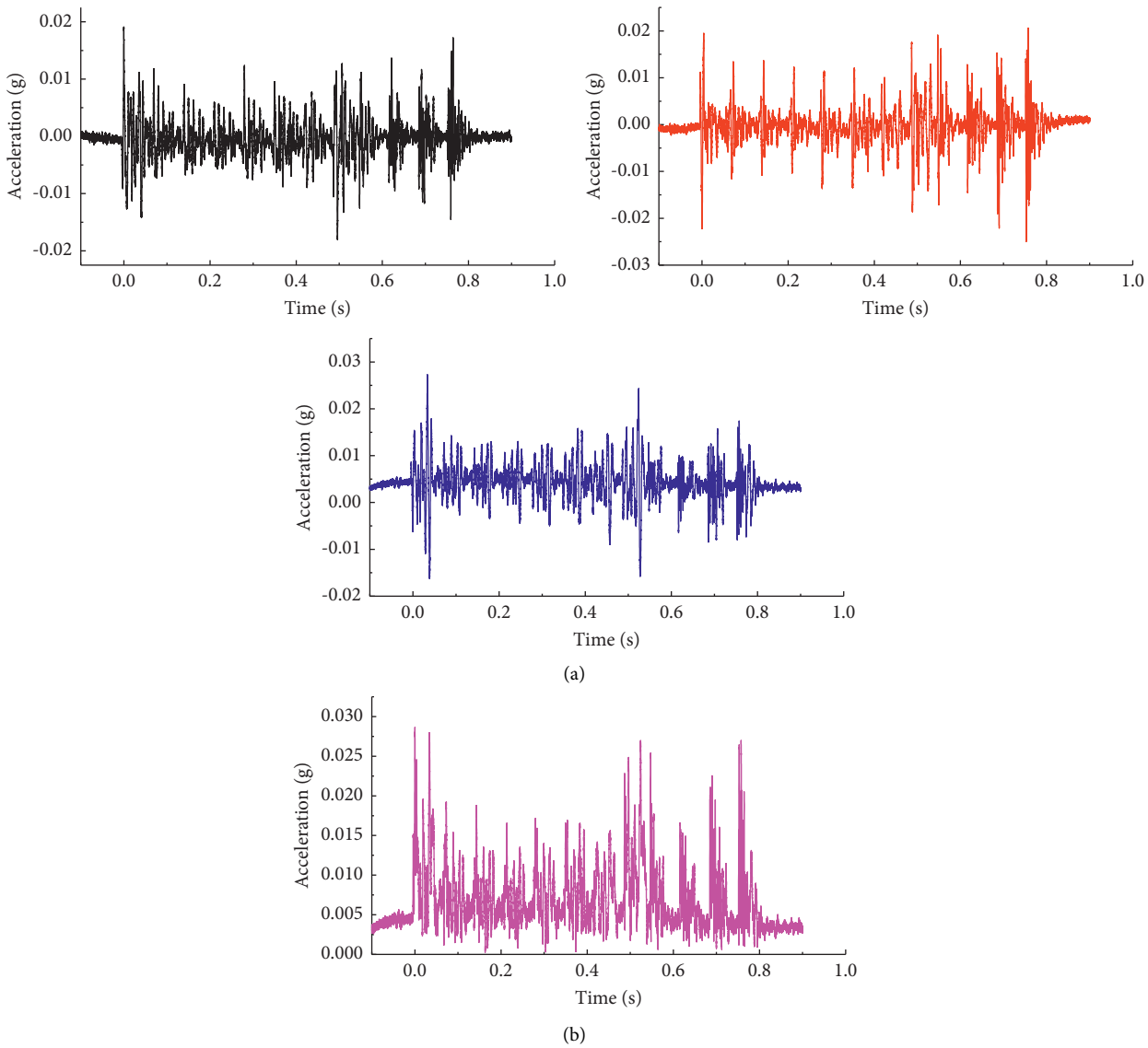

Figure 10: Acceleration waveform at 132.5 m near tunnel blasting area. (a) Three-direction waveform of blasting vibration acceleration. (b) Total acceleration waveform.

monitoring. The explosion parameters and the distance from the blasting source will affect the amplitude and frequency characteristics of the vibration field so as to further select the appropriate specification of monitoring equipment. Usually, the blasting distance range is defined by two factors: near-field and far-field vibration behaviors.

According to waveform observation results collected in blasting vibration monitoring and the dependence of amplitude on distance and source energy, this paper proposed four different monitoring fields. The proposed areas are defined by the multiple of the integral value of the maximum single section charge and distance, which is called scaled distance (SD). In the near-middle field of blasting, the correlation of the square root is better than cubic root [24, 25]. SD is calculated by dividing the distance from the blasting source by the square root of the maximum single section charge. For the near-field, due to the influence of group hole effect, it is impossible to determine the appropriate distance between the blasting source and the measuring point. Therefore, in order to facilitate subsequent analysis, it is recommended to take the horizontal distance from the measuring point to the tunnel face as the distance from the blasting source. Table 2 lists the expected peak amplitude characteristics within the specified range.

3.3. Vibration Attenuation. As can be seen from Figure 11, the blasting vibration acceleration decreases with the increase of distance, and the blasting vibration attenuation is fast in the near-field and slow in the far-field. The acceleration attenuation rate also decreases with the increase of distance. The attenuation amplitude in the near-field, especially in the extremely near-field, is much larger than that in the middle- and far-field. The rapid attenuation near the blasting area is due to the continuous expansion of the wavefront on the one hand and the absorption of medium

Table 2: Suggested definitions of tunnel blast monitoring regions.

Distance region	Maximum expected PPA (g)	Scaled distance ($m/kg^{0.5}$)
Extreme near-field	>100	SD ≤ 0.5
Near-field	10–100	0.5 < SD ≤ 2.5
Intermediate-field	3–10	2.5 < SD ≤ 7.0
Far-field	<3	SD > 7.0

Note. PPA is short for peak particle acceleration.

damping on the other hand. Rock mass medium has natural low-pass filtering. For high-frequency vibration, medium damping is large, and high-frequency components will be significantly attenuated, resulting in relatively large low-frequency components far away from the blasting source.

According to Figure 12, the vibration acceleration attenuation trend of cutting holes, caving holes, and peripheral holes is basically the same. According to the above regional division, the maximum PPA of measuring points in the extremely near-field and near-field is generated by the blasting of peripheral holes. In the far-field, the maximum PPA of the measuring point is generated by the cutting holes. The maximum PPA of the measuring point in the middle-field transits from the peripheral holes to the cutting holes.

In the near-field, due to the small distance, the energy attenuation generated by the blast holes closest to the measuring point is less than that of other blast holes, so the maximum blasting vibration acceleration is generated by the nearest peripheral holes. In the middle and far-field, because there is only one free surface on the tunnel face when cutting holes is detonated, the energy generated by the cutting hole blasting can fully spread to the rock mass, and the energy attenuation is slow, while there are two free surfaces when other blast holes are detonated, the rock clamping force is reduced, and the energy attenuation is fast. After equal-distance propagation, the residual energy carried by the cutting hole blasting is greater than that after the attenuation of other holes, which shows that in the far area of blasting, the maximum blasting vibration velocity in the surrounding rock is generated by the cutting hole blasting.

There are differences in the vibration characteristics generated in the surrounding rock by the explosion of cutting holes and peripheral holes. The attenuation rate of PPA generated by peripheral holes is faster. There are at least two reasons for this difference: firstly, there are more free surfaces when the peripheral holes are detonated, and the energy tends to be released to the nearest free surface, resulting in faster attenuation; secondly, the blasting of cutting holes and caving holes has caused a certain degree of damage to the internal rock, the expansion of micro-cracks in the rock, the decrease of strength, and the increase of discontinuities, all of which can lead to the increase of PPA attenuation rate of peripheral holes after blasting.

In the near-field, the distance is the main influencing factor, and the vibration amplitude is mainly affected by the surrounding hole blasting closest to the measuring point. In the far-field of blasting, the distance difference can be ignored, the clamping of surrounding rock plays a great role,

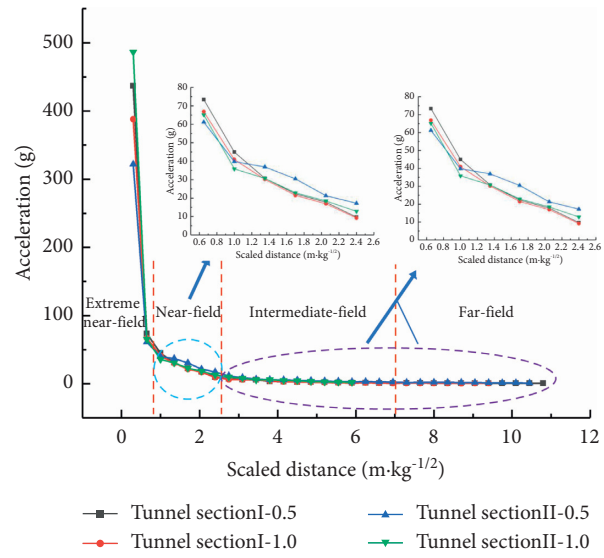

Figure 11: Vibration attenuation in different areas.

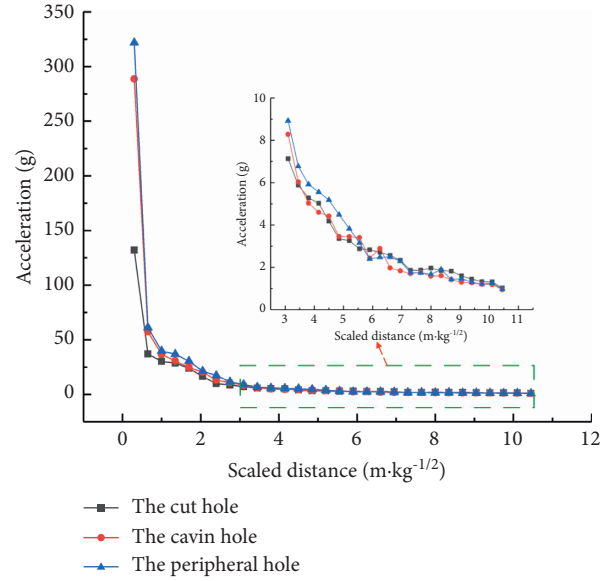

Figure 12: Attenuation curves of vibration acceleration of different blast holes.

and the vibration amplitude is mainly produced by the cutting holes with a large charge.

In the near-middle field of tunnel, the blasting vibration generated by peripheral holes is dominant, so the three-directional vibration data of peripheral holes are mainly analyzed. It can be seen from Figure 13 that the overall magnitude of three-directional vibration intensity in the near-middle region is $X > Y > Z$. The three-directional vibration intensity tends to be the same with the increase of distance. In the near-field, the main blasting vibration is body wave, which mainly affects the horizontal vibration. With the increase of distance, the influence of S wave is significantly weakened. Surface wave is generated on the free surface or medium interface and gradually increases, affecting the vibration in the vertical direction.

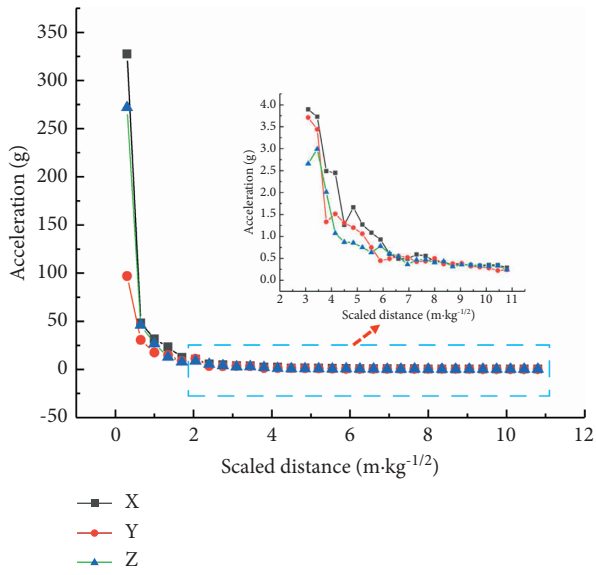

Figure 13: Three-directional acceleration curves of peripheral hole.

4. Modification of Vibration Prediction Formula

The acceleration is also recorded in three directions. The maximum value of acceleration component may not appear at the same time, but if the vibration level in any direction exceeds the specified safety limit, the structure may be damaged [26–28]. Therefore, this paper selected the longitudinal vibration with the largest vibration in three directions for analysis.

Like the velocity, the attenuation of vibration acceleration has the same form [29, 30],

$$\mathrm{PPA} = k(SD)^{-b}, \tag{1}$$

where $SD = R/Q^{1/2}$; k and b are site coefficient and attenuation coefficient, respectively; R is the distance between the blasting source and the monitoring point, m; and Q is the maximum single-period charge, kg.

Shan et al. give the calculation method of the same section charge initiation [31–33]. It is assumed that when the group charge is detonated at the same time and the distance between each charge and the measuring point is no more than 10%, the equivalent distance R and equivalent charge Q must be calculated first. The explosive quantity is the total charge of the group charge, which is then substituted into the particle vibration velocity formula to determine the particle vibration velocity caused by the group charge. The actual situation of on-site construction is possible that the tunnel face is 16.5 m wide and 7.5 m high, but the nearest horizontal distance from the measuring point to the face is only 3 m. Taking the blasting peripheral holes in the same section as an example, the blasting holes are distributed along the tunnel contour, and the distance between blasting holes is several times that from the measuring point to the face. The blasting hole depth and the distribution position of each section of blasting holes on the tunnel face greatly affect the blasting center distance. The blasting holes in the same section are too scattered, which makes it impossible to treat the tunnel face explosion as a centralized blasting source. Therefore, it is recommended to take the horizontal distance from the measuring point to the tunnel face as the distance from the explosion source.

Through the analysis of a typical waveform, two temporary caving holes are added between the fourth section and the fifth section of caving holes in the right half of the tunnel face. The single period charge is only 4.8 kg, but the actual vibration intensity is higher than the cutting holes with a single section charge of 52.8 kg. This shows that the vibration intensity in the near blasting field is more sensitive to distance. In the near blasting area, using Sadovsky's formula to predict will overestimate the effect of charge and weaken the influence of distance. Therefore, in order to reflect the actual situation in the near area of tunnel blasting, it is necessary to modify the traditional formula, increase the correction index and correlation coefficient in the near-field, and put forward the regression and prediction formula of vibration in the near-field of blasting with reference to Ghosh's formula [34], which is as follows:

$$\mathrm{PPA} = k(SD)^{-\alpha} e^{\beta(\sqrt{HD}/Rl/R)}, \tag{2}$$

where Q is the maximum single-stage dosage, kg; R is the vertical distance between the measuring point and the tunnel face, m; H is the tunnel height, m; D is the tunnel width, m; L is the depth of cyclic footage, m; l is the coefficient and attenuation coefficient related to the topography and geology of the blasting area; and β is the coefficient related to the blasting holes distribution and blasting holes depth in the tunnel face.

A total of 31 blasting tests were conducted in the first stage of this test. Due to the difference of rock conditions in each construction cycle, the parameters such as the total charge used in actual blasting or the total charge of blasting holes in each section are different. A large number of data results were measured under the conditions of different charge quantities and different blasting center distances. Due to space limitations, some vibration monitoring data are listed in Table 3.

The multiple regression fitting of (1) and (2) was carried out by using the vibration data to obtain the empirical formula characterizing the propagation and attenuation law of blasting vibration, as shown in equations (3) and (4).

$$\mathrm{PPA} = 696\left(\frac{Q^{1/2}}{R}\right)^{-1.55}, \quad \left(R^2 = 0.82\right). \tag{3}$$

It can be seen from (3) and (4) that the correlation coefficient of the correction formula is the largest; that is, the fitting correlation is the best, which shows that the formula can accurately reflect the change law of the near-field of the tunnel by introducing the correction index and correlation coefficient in the tunnel near-field. The predicted vibration velocity is calculated by using the fitting results of the above two formulas. Comparing the velocity with five groups of field measured data, the relative error and average relative error between the predicted value and the measured value can be obtained, as shown in Table 4.

Table 3: Partial vibration acceleration data.

Horizontal distance from measuring point to tunnel face (m)	Maximum single-stage charge (kg)	SD ($m \cdot kg^{-1/2}$)	PPA ($m \cdot s^{-2}$)
3.0	89.4	0.32	4366
6.5	129.6	0.57	733
10.0	101.9	0.99	1321
13.5	115.3	1.26	307
17.0	110.5	1.62	170
20.5	110.2	1.95	1011
24.0	106.7	2.32	86
27.5	124.4	2.47	322
31.0	85.3	3.36	163
34.5	81.9	3.81	58
38.0	97.5	3.85	396
41.5	104.6	4.06	30
45.0	104.9	4.39	149
48.5	115.2	4.52	22

Table 4: Comparison between measured vibration velocity and predicted vibration velocity in the near blasting area of Zhaitang tunnel.

Formula	Measured data	Acceleration ($m \cdot s^{-2}$)				
		2235	418	330	303	236
Formula (1)	$A_{prediction}$	1882	346	281	263	187
	Relative error (%)	15.8	17.2	14.8	13.2	20.7
Formula (2)	$A_{prediction}$	2443	381	304	324	219
	Relative error (%)	9.3	8.8	8.4	6.9	7.2

$$\mathrm{PPA} = 315\left(\frac{Q^{1/2}}{R}\right)^{-0.19} e^{-0.26\left(\sqrt{7.5*16.5}/R*3.5/R\right)}, \quad \left(R^2 = 0.88\right). \tag{4}$$

It can be seen from Table 4 that the relative error between the predicted value and the measured value of the modified formula is less than 10%, and its prediction accuracy is high, which indicates that it is more accurate to predict the blasting vibration velocity for near-field blasting in the tunnel. Also, using (2) to calculate the blasting vibration velocity, the group hole effect of blasting holes on the tunnel face and influencing factors of blasting hole length can be considered.

5. Conclusions

Through the vibration test of the acceleration sensor installed in the surrounding rock near the tunnel face of Zhaitang Tunnel, the New Line Expressway of China National Highway 109, the following conclusions can be drawn:

(1) By observing the typical waveform of blasting vibration, it is found that the vibration waveform in the near-field has the characteristics of obvious segmentation, short duration, high frequency, and large amplitude; the far-field vibration waveform overlaps with long duration, low frequency, and small amplitude.

(2) The attenuation of tunnel blasting vibration is fast in the near-field and slow in the far-field, and the attenuation rate decreases with the increase of distance. In the extremely near-field and near-field of blasting, the maximum PPA of measuring points is generated by peripheral hole blasting; in the far-field of blasting, the maximum PPA of the measuring point is generated by the cutting hole. In the near-middle field, the overall magnitude of three-directions vibration intensity is X direction > Y direction > Z direction. With the increase of distance, the three-dimensional vibration intensity tends to be the same.

(3) The prediction formula of blasting vibration suitable for the near-field of the tunnel is modified, and its engineering application feasibility is verified. The next step is to study its applicability in the near blasting area of open-pit mine.

Data Availability

The data used to support the findings of this study are available from the corresponding author upon request.

Conflicts of Interest

The authors declare that there are no conflicts of interest regarding the publication of this article.

Acknowledgments

This work was supported by the Natural Science Foundation of Shandong Province (ZR2020QE266), the Fundamental Research Funds for the Central (2017QL05), the National Key Basic Research Development Program ("973 Program") Project (2014CB047000), and the National Key R&D Program (2017YFC0804607).

References

[1] G. L. Yang, P. Rocque, and W. F. Bawden, "Measurement and analysis of near- field blast vibration and damage," *Geotechnical & Geological Engineering*, vol. 12, no. 2, pp. 169–182, 1994.

[2] W. Shen, G. Shi, Y. Wang, J. Bai, R. Zhang, and X. Wang, "Tomography of the dynamic stress coefficient for stress wave prediction in sedimentary rock layer under the mining additional stress," *International Journal of Mining Science and Technology*, vol. 31, no. 4, pp. 653–663, 2021.

[3] J. Ma, X. L. Li, J. G. Wang et al., "Experimental study on vibration reduction technology of hole-by-hole presplitting blasting," *Geofluids*, vol. 20, pp. 271–284, 2021.

[4] J. Wang, T. Zuo, X. Li, Z. Tao, and J. Ma, "Study on the fractal characteristics of the pomegranate biotite schist under impact loading," *Geofluids*, vol. 22, pp. 166–179, 2021.

[5] R. Holmberg and P. A. Persson, "The Swedish Approach to Contour Blasting," in *Proceedings of the Conference on Explosives and Blasting Technique (CDROM)*, pp. 113–126, ISEE, Cleveland, OH, USA, 1978.

[6] G. Kelly, *Near-field Blast Vibration Monitoring and Analysis for Prediction of Blast Damage in Sublevel Open Stoping*, Curtin University of Technology, Perth, Western Australia, 2010.

[7] Q. Zhang, L. Li, S. Li, W. Ding, and W. Hong, "Experimental study of blasting dynamic vibration of closely adjacent tunnels," *Rock and Soil Mechanics*, vol. 29, no. 10, pp. 655–660, 2008.

[8] J. Zhang, "Vibration characteristics of blasting in bed rock mass at sanxia project," *Explosion and Shock Waves*, no. 2, pp. 131–137, 2001.

[9] J. Zhang and Q. Peng, "Field experiment and its analyses of attenuation law for seismic waves resulting from rock blasting," *Journal of Liaoning Technical University*, vol. 20, no. 4, pp. 399–401, 2001.

[10] H. Ye, Z. Yue, and X. Yang, "Experimental study on energy propagation law of blasting vibration signals for tunnel lining concrete," *Science Technology and Engineering*, vol. 19, no. 18, pp. 296–301, 2019.

[11] H. Fu, Y. Zhao, J. Xie, and Y. Hou, "Study of blasting vibration test of area near tunnel blasting source," *Chinese Journal of Rock Mechanics and Engineering*, vol. 30, no. 2, pp. 335–340, 2011.

[12] H. Fu, "Study on the stability of the surrounding rock of blasting construction tunnel," *China Railway Science*, vol. 32, 2011.

[13] H. Fu, H. Kong, and J. Wu, "Controlled technology of tunnel blasting in complex environment," *China Civil Engineering Journal*, vol. 50, no. 2, pp. 286–291, 2017.

[14] Z. Zhang, "Prediction of blasting vibration of area near tunnel blasting source," *Explosion and Shock Waves*, vol. 34, no. 3, pp. 367–372, 2014.

[15] F. Xie, L. Han, D. Liu, and L. I. Chen, "Vibration law analysis for a tunnel's field near blasting based on waveform superposition theory," *Journal of Vibration andShock*, vol. 37, no. 2, pp. 182–188, 2018.

[16] F. Xie, L. Han, and D. Liu, "Prediction method on tunnel blasting vibration near explosive source field based on waveform superposition theory," *Blasting*, vol. 34, no. 3, pp. 151–156, 2017.

[17] L. Han, *Experimental Study on Vibration Effect of Deep Hole Bench Blasting in Near Field*, China University of Mining and Technology, Beijing, China, 2016.

[18] L. Han, C. Xin, S. Liang, and D. Liu, "Experimental study on vibration characteristics of deep hole bench blasting in both near and far field," *Journal of Vibration and Shock*, vol. 36, no. 8, pp. 65–70, 2017.

[19] L. I. Yang, Y. Ren, S. Peng Syd, H. Cheng, N. Wang, and J. Luo, "Measurement of overburden failure zones in close-multiple coal seams mining," *International Journal of Mining Science and Technology*, vol. 31, no. 1, pp. 43–50, 2021.

[20] L. A. Ismail, S. Kwon, H. O. Sakiru, and I. M. Adebayo, "Blast-induced ground vibration prediction in granite quarries: an application of gene expression programming, ANFIS, and sine cosine algorithm optimized ANN," *International Journal of Mining Science and Technology*, vol. 31, no. 2, pp. 265–277, 2021.

[21] X. Sun, C. Zhao, Y. Zhang, F. Chen, S. Zhang, and K. Zhang, "Physical model test and numerical simulation on the failure mechanism of the roadway in layered soft rocks," *International Journal of Mining Science and Technology*, vol. 31, no. 2, pp. 291–302, 2021.

[22] R. Hafeezur, N. Abdul Muntaqim, W. Ali, J. Muhammad, A. Abdullah Rini, and H. Yoo, "Numerical evaluation of new Austrian tunneling method excavation sequences: a case study," *International Journal of Mining Science and Technology*, vol. 30, no. 3, pp. 381–386, 2020.

[23] M. Wang, T. Ge, C. Qi, and Q. Qian, "Study of deformation and failure of rock under explosion load (partI)," *Journal of Disaster Prevention and Mitigation Engineering*, no. 2, pp. 43–54, 2003.

[24] O. Dogan, Ö. Anil, S. O. Akbas, E. Kantar, and R. Tuğrul Erdem, "Evaluation of blast-induced ground vibration effects in a new residential zone," *Soil Dynamics and Earthquake Engineering*, vol. 50, pp. 168–181, 2013.

[25] J. Yang, J. Cai, C. Yao, P. Li, Q. Jiang, and C. Zhou, "Comparative study of tunnel blast-induced vibration on tunnel surfaces and inside surrounding rock," *Rock Mechanics and Rock Engineering*, vol. 52, no. 11, pp. 4747–4761, 2019.

[26] X. L. Li, S. J. Chen, Z. H. Li, and E. Y. Wang, "Rockburst mechanism in coal rock with structural surface and the microseismic (MS) and electromagnetic radiation (EMR) response," *Engineering Failure Analysis*, vol. 124, no. 6, pp. 381–396, 2021.

[27] X. L. Li, S. J. Chen, Q. M. Zhang, X. Gao, and F. Feng, "Research on theory, simulation and measurement of stress behavior under regenerated roof condition," *Geomechanics and Engineering*, vol. 26, no. 1, pp. 49–61, 2021.

[28] X. l. Li, S. J. Chen, S. M. Liu, and Z. H. Li, "AE waveform characteristics of rock mass under uniaxial loading based on Hilbert-Huang transform," *Journal of Central South University*, vol. 28, no. 6, pp. 1843–1856, 2021.

[29] S. Yang, "Vibration law and safety estimate of the tunnel subjected to blasting," *Explosion and Shock Waves*, vol. 5, no. 4, pp. 17–23, 1985.

[30] S. Yang and Z. Ding, "Vibration laws of cavity in rock subjected to adjacent blasting," *Explosion and Shock Waves*, vol. 3, no. 4, pp. 33–43, 1983.

[31] R. Shan and L. Song, "Model test studies of damage evaluation of frozen rock wall under blasting loads," *Chinese Journal of Rock Mechanics and Engineering*, vol. 33, no. 10, pp. 1945–1952, 2014.

[32] Y. Xue and Y. Yao, "Effect of topographical condition on distribution of blasting vibration velocity," *Metal Mine*, no. S1, pp. 434–437, 2009.

[33] Y. Gun, "Discussion on the utilization of blasting vibration formula," *Blasting*, vol. 26, no. 4, pp. 78–80, 2009.

[34] I. Arellano and V. Roncero, "Simple new blast vibration predictor (based on wave propagation laws)," in *Proceedings of the 24th US Symposium on Rock Mechanics*, College Station, TX, USA, June 1983.